MICROCOPY RESOLUTION TEST CHART

JREAU OF STANDARDS 1963-A

Performance of Polymer Electrolyte

Cells at +25 to +100°C

M.Z.A. Munshi

B.B. Owens

Department of Chemical Engineering and Materials Science

Corrosion Research Center

221 Church Street, SE

Minneapolis, MN 55455

ABSTRACT

Solid state rechargeable polymer electrolyte batteries utilizing lithium anodes and V_6O_{13} composite cathodes were investigated at 100°C. The polymer electrolyte was a complex formed between polyethylene oxide (PEO) and $LiCF_3SO_3$. Over a hundred cycles were obtained at the C/5 rate (45% depth of discharge) with greater than 75% of the initial capacity of V_6O_{13} being maintained at cycle number one-hundred. Cells made with propylene carbonate (PC) doped polymer electrolyte also showed good performance at room temperature.

88 4 26 14 9

1. INTRODUCTION

Ionically conducting polymers were discovered by Fenton et al. in 1973 [1]. They showed that complexes formed between polyethylene oxide (PEO) and various alkali metal salts exhibited high ionic conductivities at elevated temperatures. This was followed by Armand's proposal for an all-solid-state lithium battery [2]. Subsequently a large number of groups have shown interest in the application of this polymeric solid electrolyte [3-5].

The attractive mechanical and electrical properties ($\sigma \sim 10^{-4}$-10^{-3} $(\Omega cm)^{-1}$ at 100-140°C) of these polyether complexes resulted in further investigation on ionically conducting polymers [6-13]. However their application to solid state batteries has not been fully documented. There are only a few instances on the use of these polymer electrolytes in practical demonstration cells [14-17].

The prime objective of the development program in polymeric batteries is to develop a stable battery with the ability to store and to deliver energy efficiently and economically. The group at Hydro-Quebec, Canada and France operate their cells at 80-100°C whilst those at Harwell, England operate at 120-140°C. Current densities of 0.1-1.0 $mAcm^{-2}$ have been reported for PEO-LiCF$_3$SO$_3$ electrolyte cells with energy efficiencies and specific powers of 70-80% and 100-300 Wdm^{-3}, respectively [14,17]. Furthermore over 100 cycles have been claimed by the Harwell workers [14]. However, no detailed accounts appeared in the literature. In addition, the scaling-up of these cells have been rather slow.

Recently the Canadian-French group have found a new family of polyether electrolytes that could be used for room temperature lithium cells [17]. Current drains of 3-20 μAcm^{-2} were demonstrated for MnO_2-based primary and MoO_2-based secondary systems. It would be highly desirable if the V_6O_{13} cathode could also be used for room temperature operations in solid state batteries, not only from the fact that up to 8 Li can be inserted into its structure but also because it is lightweight and has a high voltage.

In this paper we report results for $Li|(PEO)_8 \cdot LiCF_3SO_3|V_6O_{13}$ cells operating between +25 to +100°C.

2. EXPERIMENTAL

2.1 Preparation of the Cell Material

The fabrication of the cell and handling of all materials were carried out in a < 1% R.H. dry room. The polymer electrolyte was prepared by dissolving a known weight of $LiCF_3SO_3$ in acetonitrile (dried using molecular sieve) followed by a known weight of PEO (M.W. 5 x 10^6) with constant stirring (both solid reagents pre-dried at 50°C for several days). The weights used were such that the final PEO:Li salt ratio was 8. The solution was stored in a sealed bottle for 2-5 days to homogenize.

Large areas of bubble free films were obtained by a solution casting technique using a doctor blade. The films were dried in the dry room air for two days, followed by careful stringent drying under

vacuum over P_2O_5 for two weeks or more. Film thickness were of the order of 10-20 μm.

The process for preparation of the cathode incorporated the materials V_6O_{13}, Shawinigan Black, PEO, lithium salt and acetonitrile. The cathode was prepared by a complex procedure resulting from a study involving the milling process, process times, particle size and method of introduction of the lithium salt and PEO [18]. Shawinigan Black was added to enhance the electronic conductivity of the V_6O_{13} active material. The electrolyte phase was added to enhance the ionic conductivity and also to increase the plasticity of the cathode. Cathodes were cast from the resultant dispersions directly onto aluminum or nickel foil current collectors ($\simeq$ 17 μm), also using the doctor blade technique. Films in the 10-25 μm range were obtained.

Anode discs were cut from lithium foils (50 μm thick) obtained from Foote Mineral Co.

2.2 Cell Construction

2.86 cm diameter cell. Small cells were assembled in the dry room as shown in Figure 1. The geometrical surface area of the electrolyte, lithium and cathode was effectively 6.4 cm^2. Concentric cut polypropylene spacers were used to separate the two electrodes. Two electrolyte layers of about 10 μm were employed in each cell. The cells were sandwiched between stainless steel plate current collectors and maintained under a constant pressure using a clamping system. They were placed in an oven at 100°C.

10 cm diameter cell. Larger cells were fabricated with a geometrical area of 75 cm². The capacity loading and hence the thickness of the cathode was maintained constant between 20-25 μm in order to keep the capacity of each cell the same. The cells were constructed in much the same way as the smaller designs and scaled-up in a parallel connection.

1 cm diameter cell. The room temperature cells were assembled in the glove box. The diameter of the electrolyte was 1 cm and the thickness 50 μm. A polypropylene spacer with a 1 cm diameter void for the electrolyte was used to separate the cathode and the lithium. Once the electrolyte and the spacer were in place, a known amount of propylene carbonate was added to the electrolyte using a micropipette. This was allowed to absorb well into the electrolyte before placing the lithium electrode. In this case the cell was sandwiched between two glass slides to maintain even pressure and was hermetically sealed using epoxy.

All cells were cycled in the glove box. The theoretical capacity of the cathode was based on 8 Li intercalating into the V_6O_{13} structure. The electrode loading was about 18-2 mAhcm^{-2} for cells operating at 100°C and 0.5 mAhcm^{-2} for cells operating at room temperature.

In all cases a constant current discharge and a constant voltage charge through a limiting resistor were employed.

3.   RESULTS AND DISCUSSION

Most of the cells without PC demonstrated an initial open-circuit voltage of over 3.5 V at room temperature. However, heating to 100°C reduced this value to 2.9-3.1 V.   The PC cells made for room temperature operation had open-circuit voltages varying between 3.12 and 3.27 V.

Figure 2 shows typical families of discharge voltage curves for a nominal 3 V, 13 mAh cell at various rates of discharge from the 40 h rate to the 1 h rate at a temperature of 100°C. The discharges were carried out at constant current to +1.8 V. As noted previously [], several plateaus are apparent in the voltage-time plots and these are characteristic of the change in the oxidation state of the V_6O_{13} cathode during discharge. During recharge there is a loss in capacity compared to the initial discharge.

Figure 3 shows a plot of the theoretical capacity versus the number of cycles for small-scale cells at 100°C. Ironically, although our methods of cell manufacture were different to the Harwell group, we seem to obtain similar trends in the result. At low rates of discharge, the initial capacity is considerably larger than at high rates. Furthermore, the decline in capacity is much faster at low rates than at high rates (cf C/20 and C/10 vs C/5). Greater stabilization occurs at the higher rate of discharge. At first sight this seems rather unusual and we have no sound explanation for this effect. However, our results are consistent with the work of Hooper and North [].

Table 1 shows the variation of the discharge voltage against the iR drop at different cycling rates. The initial iR drop was calculated to be predominantly due to the solid electrolyte. However, as the discharge proceeds, more and more lithium ions are inserted into the V_6O_{13} structure. Consequently, the iR drop increases and this is interpreted as due to a combination of the changes taking place at the cathode as well as the transport of counter ions through the electrolyte. It is envisaged that the motion of counter ions in the electrolyte would lead to some kind of film formation which may be less conducting than the initial electrolyte. The constancy in the capacity corresponds to a stabilization in the iR drop. This change in the iR drop during discharge might also be responsible for the gradual decline in the voltage-time curves (Figure 2).

The stabilization in the capacity with cycling is greatest for the cell operating at the C/5 discharge rate. In this case a hundred cycles were obtained with greater than 75% of the initial utilization of V_6O_{13} being maintained at cycle number 100. Post-mortem examination of the cell using optical microscopy has shown the Li-electrolyte-cathode interface to be well intact []. In all cases the cell materials indicate good adhesion at the anode|electrolyte and electrolyte|cathode interfaces even after 100 deep cycles. The structures of the lithium, electrolyte and cathode become finer grained and hence smoother. In addition, there was no evidence of dendrites at the lithium electrode in any of the cells examined.

As the cycling progresses, the coulombic efficiency approaches almost 100%. These encouraging results led us to believe that if such performance can be achieved for smaller cells at current densities of 0.1-0.4 mAcm^{-2} and with significant utilization of the cathode, then it may be possible to scale-up the system for larger battery applications.

Figure 4 shows the performance of the scaled-up 10 cm cells. Initially considerable problems were encountered resulting in poor capacities and this was generally due to the method of constructing the cells. However the use of sharp toolings to cut the cast films and greater care taken in the cell construction vastly improved the cell performance.

Cells scaled-up to about 150 mAh behaved in the same way as the smaller designs. The coulombic efficiency was between 90-100% except for the initial cycle. Stabilization was also observed to be greater at the higher rates of discharge than at the lower rates. However a cell scaled-up to about 480 mAh capacity failed to perform well on a couple of occasions and no attempt was made to investigate the problem. The only explanation that could be worthy of proposal is the extreme difficulty in constructing ultra large area flat cells using such thin electrode/electrolyte materials.

Due to this occurrence, cells were scaled-up by assembling several 150 mAh size in a parallel connection. Up to the present time, five such cells have been connected in parallel giving a total capacity of 750 mAh. The discharge rates used were between C/50 and C/20 giving current outputs of 15-37.5 mA. Higher rates resulted in severe

polarization. As Figure 4 shows capacity of over 60% theoretical is possible at the C/50 rate with stabilization occurring after about six cycles. Only about 30% constant capacity is obtained at the C/20 rate. Despite the low capacities compared to the smaller size cells at the same rate, these first results are signs of encouragement. Nonetheless, considerable improvement in performance is necessary with these kinds of systems if they are to be used for practical applications.

Figure 5 depicts the performance of room temperature cells operating at a nominal discharge current of $10\mu A$ [19]. The cell with zero percent PC additive polarized instantly even when the electrolyte thickness was reduced to 5 μm. In contrast cells containing PC were able to discharge and deliver an appreciable amount of capacity depending upon the extent of PC addition.

With 10 vol. %PC, an initial capacity of 64% is obtained. However, there is a gradual decline in capacity with cycling. Only 22 cycles are obtained before the cell capacity reaches below the 20% theoretical level.

The decline in capacity with cycling is more rapid when 40 vol. %PC is added to the electrolyte. After 12 cycles, the cell finally shorted.

The most optimum result is obtained with 20 vol. %PC. The initial capacity reaches as high as 86% theoretical. The decrease in capacity with cycling is also considerably less rapid than for either of the two

previous cases. Up to 26 cycles could be obtained before a significant decrease is apparent in the capacity.

The addition of PC to the electrolyte appears to have a marked effect on the performance of the cells. The overall effect is to increase the dielectric property (and hence the ionic conductivity) of the electrolyte. Too little solvent does not raise the conductivity high enough to produce cells with reasonable outputs. Too much PC (40 vol. %) also results in reduced cell capacities and this is probably due to the breaking up of the cathode film structure from the aluminum substrate. The best result is obtained with 20 vol. % PC. These results indicate that it is possible to cycle polymer electrolyte cells at room temperature with appropriate amounts of dopant.

Figure 6 shows a family of discharge curves for the cell containing 20 vol. % PC in the electrolyte. Even at room temperature discharge rates of up to 100 μAcm^{-2} are possible with good cycling and good rechargeability.

With greater optimization, the application of these rechargeable cells operating at room temperature is far reaching. It is quite possible to construct cells as thin as 100 μm. Such systems could be well suited for use in "smart" credit cards, standby power in uninterruptible power supplies, integrated power supplies for microelectronics and reserve power for solar cells.

Further work is under evaluation to increase the lifetime and power output of these cells. Other solvents are also being investigated in order to increase the efficiency of the cell.

REFERENCES

1. B.E. Fenton, J.M. Parker and P.V. Wright, Polymer, 14, 589 (1973).

2. M. Armand, J.M. Chabagno and M. Duclot, in: "Fast Ion Transport in Solids," eds. P. Vashista, J.N. Mundy and G.K. Shenoy (North-Holland, Amsterdam), 131, (1979).

3. J.R. Owen in "Solid State Batteries," eds. C.A.C. Sequeira and A. Hooper, NATO ASI Series, (Martinus Nijhoff Publishers), 413, (1985).

4. T.A. Skotheim and O. Inganis, J. Electrochem. Soc., 132, 2116, (1985)

5. J.M. North, C.A.C. Sequeira, A. Hooper and B.C. Tofield, Int. Meeting on Li Batteries, Abs. #32, Rome, (1982).

6. M. Stainer, L.C. Hardy, D.H. Whitmore and D.F. Shriver, J. Electrochem. Soc., 131, 784, (1984).

7. P. Ferloni, G. Chiodelli, A. Magistris and M. Sanesi, Solid State Ionics, 18 and 19, 265, (1986).

8. C.D. Robitaille and D. Fauteux, J. Electrochem. Soc. 133, 315, (1986).

9. T. Hibma, Solid State Ionics, 9 and 10, 1101, (1983).

10. J.E. Weston and B.C.H. Steele, Solid State Ionics, 2, 347 (1981).

11. M. Minier, C. Berthier and W. Gorecki, Solid State Ionics, 9 and 10, 1125, (1983).

12. P.R. Sorensen and T. Jacobsen, Polymer Bull., $\underline{9}$, 47, (1983).

13. R. Dupon, B.L. Papke, M.A. Ratner, D.H. Whitmore and D.F. Shriver, J. Am. Chem. Soc., $\underline{104}$, 6247, (1982).

14. A. Hooper and J.M. North, Solid Stat Ionics, $\underline{9}$ and $\underline{10}$, 1161, (1983).

15. J.M. North, T.L. Markin, A. Hooper and B.C. Tofield, 2nd Int. Meeting on Li Batteries, Abs. #19, Paris, (1984).

16. M. Gauthier, P. Ricoux and M.B. Armand, Proc. 2nd Int. Meeting on Li Batteries, Paris, (1984).

17. M. Gauthier, D. Fauteux, G. Vassort, A. Belanger, M. Duval, P. Ricoux, J.M. Chabagno, D. Muller, P. Rigaud, M.B. Armand, and D. Deroo, J. Electrochem. Soc., $\underline{132}$, 1333, (1985).

18. B.B. Owens, G. Martinez, results to be published.

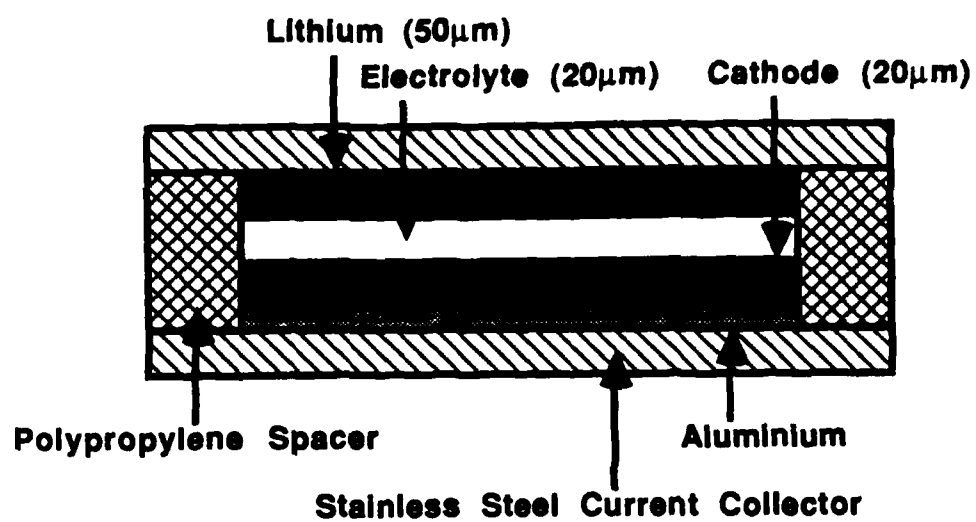19. M.Z.A. Munshi and B.B. Owens, results to be published in IEEE.

Figure Captions

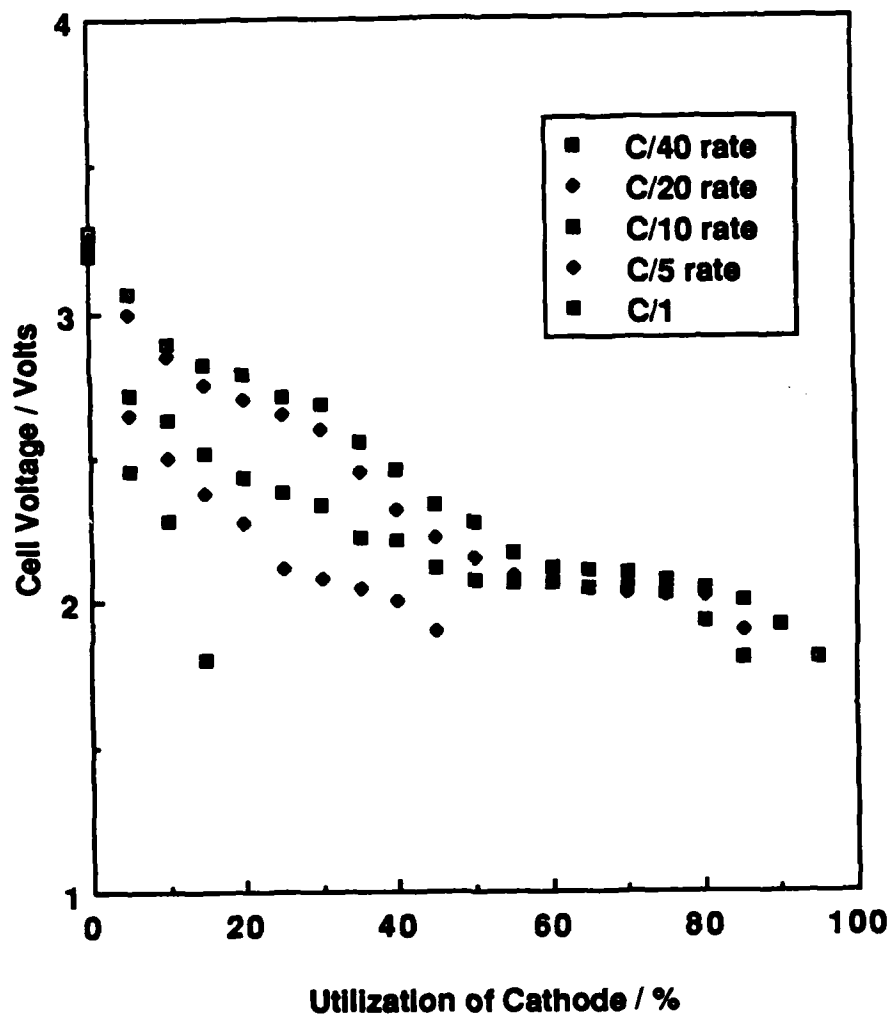Figure 1. Schematic of the polymer electrolyte cell.

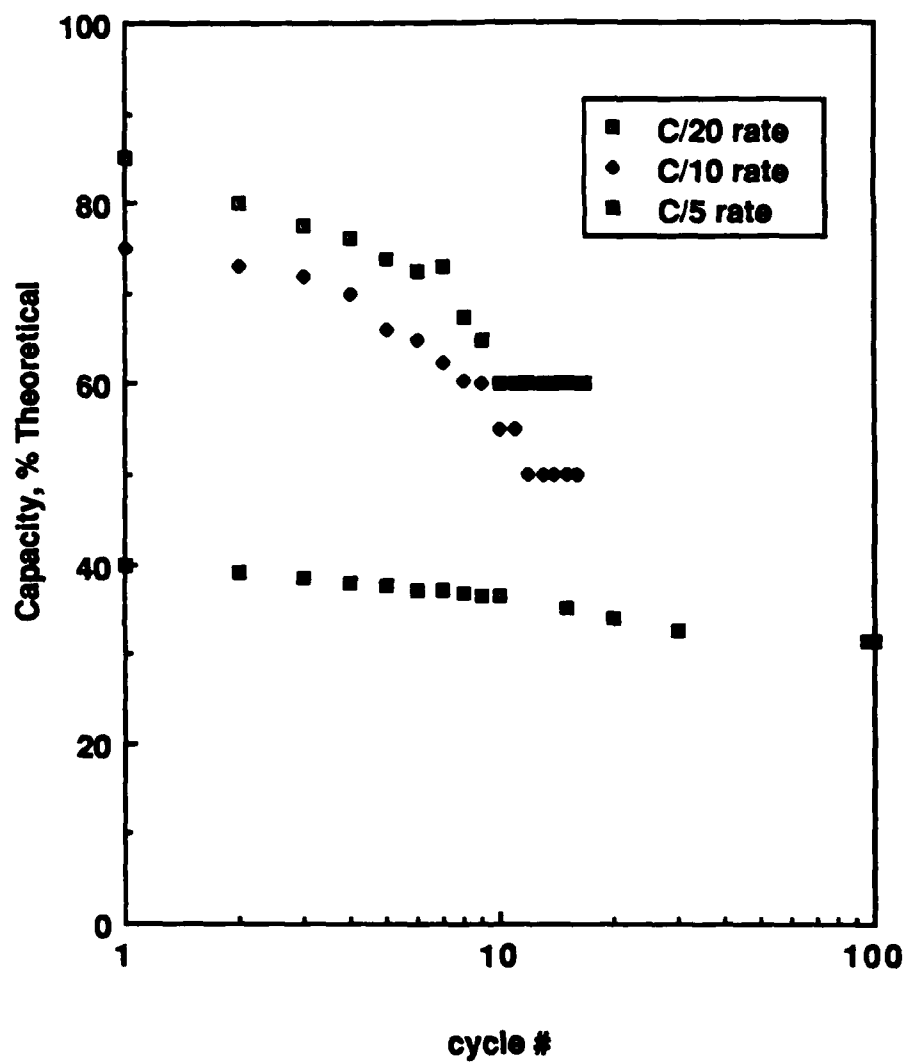Figure 2. Typical family of discharge curves at 100°C.

Figure 3. Plot of theoretical capacity versus cycle # for cells at 100°C.

Figure 4. Performance of scaled-up cells.

Figure 5. Performance of Li polymer electrolyte cells at the C/50 rate and room temperature (Ref. 19).

Figure 6. Family of discharge curves of cells containing 20 vol.% PC in the electrolyte (Ref. 19).

Table 1. Variation in the discharge voltage versus iR drop/cell at different cycling rates (cell capacity = 10.80mAh).

Discharge Voltage (volts)	iR Drop/mV			
	C/5	C/10	C/20	C/40
Initial drop	59	30	10	6
2.90	64	31	11	7
2.80	68	33	13	8
2.70	73	35	14	9
2.60	75	35	14	9
2.50	79	35	15	9
2.40	86	38	17	10
2.30	89	43	18	11
2.20	92	44	19	12
2.10	97	45	19	12
2.00	101	45	19	12
1.90	104	46	20	13
1.80	112	52	21	14

Figure 1. Schematic of the polymer electrolyte cell.

Figure 2. Typical family of discharge curves at 100°C.

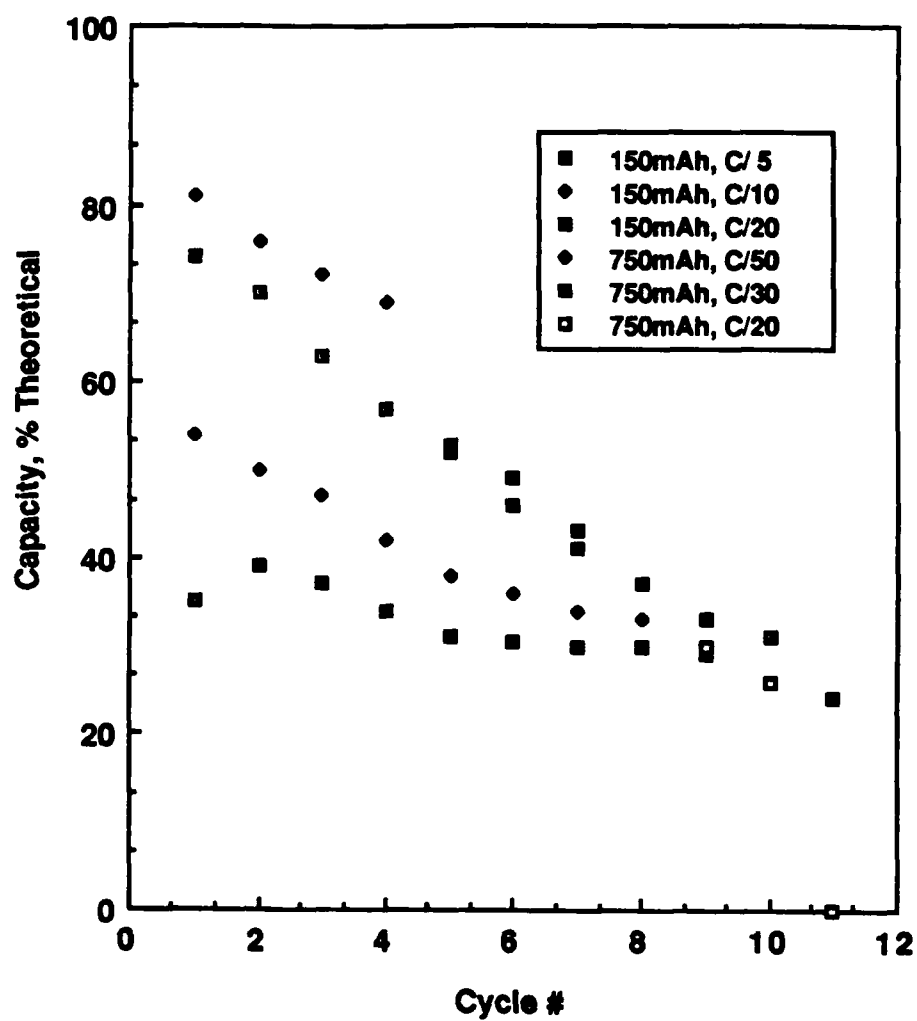Figure 3. Plot of theoretical capacity versus cycle # for cells at 100°C

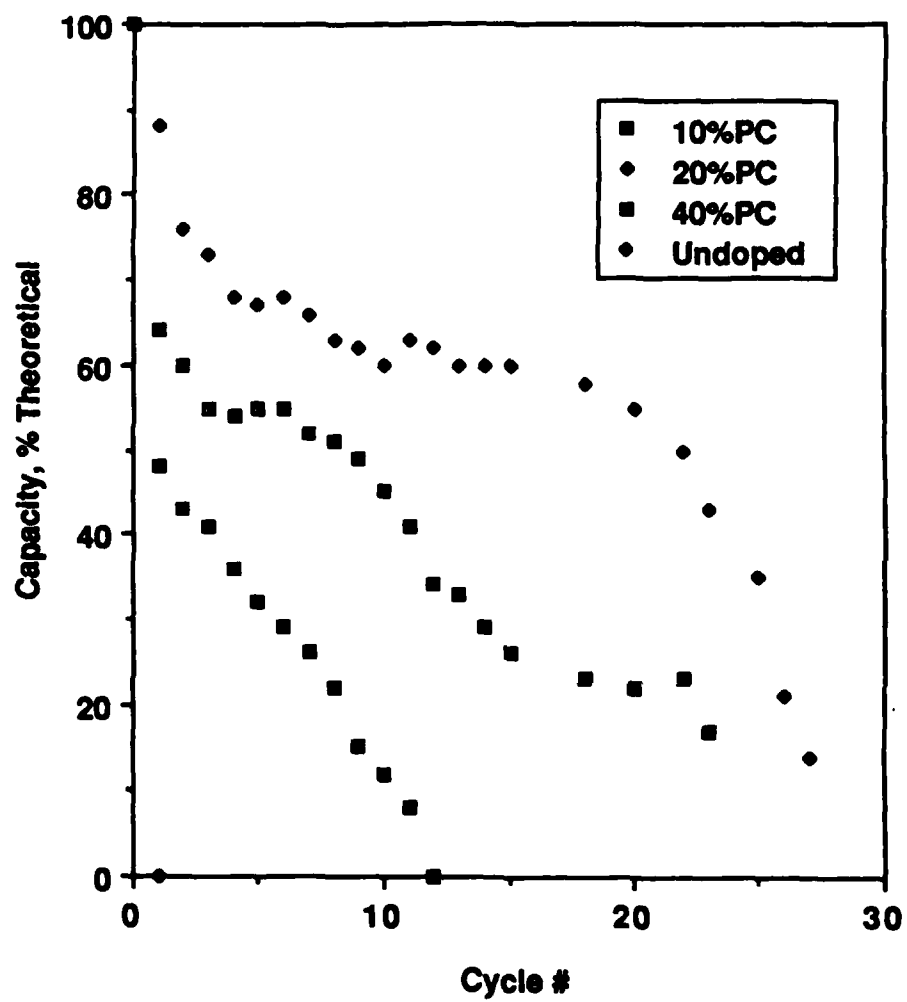Figure 4. Performance of scaled-up cells.

Figure 5. Performance of Li polymer electrolyte cells
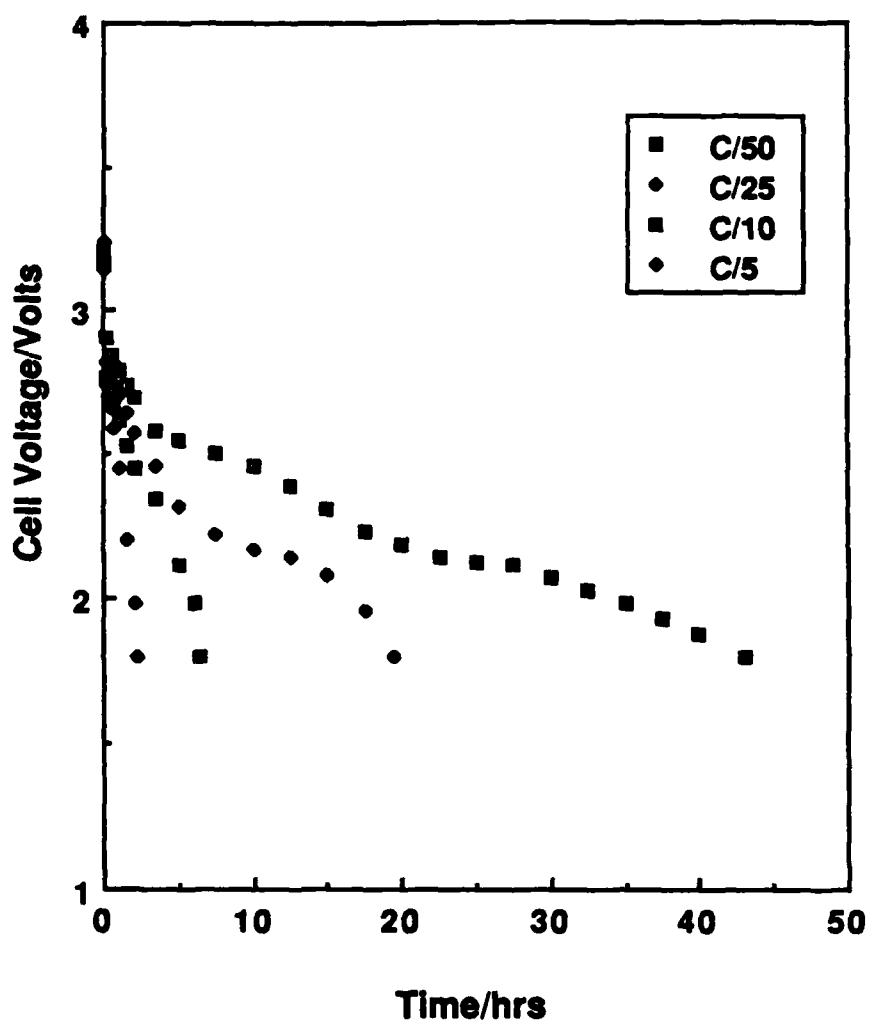at the C/50 rate and room temperature (Ref. 19).

Figure 6. Family of discharge curves for cells
containing 20 vol.% PC in the electrolyte (Ref. 19).

END

DATE
FILMED

8-88

DTIC